IEEE Photonics Journal
An IEEE Photonics Society Publication

Open Access

Broadband Polarization Beam Splitter by Using Cascaded Tapered Bent Directional Couplers

Volume 11, Number 4, August 2019

Ning Zhao
Ciyuan Qiu
Yu He
Yong Zhang
Yikai Su

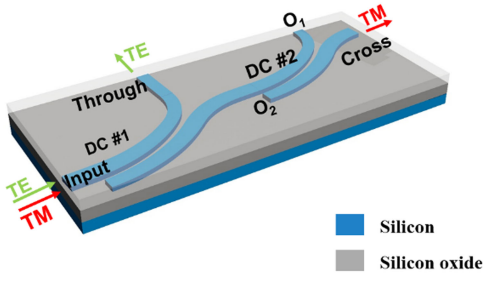

DOI: 10.1109/JPHOT.2019.2920909
1943-0655

Broadband Polarization Beam Splitter by Using Cascaded Tapered Bent Directional Couplers

Ning Zhao, Ciyuan Qiu, Yu He, Yong Zhang, and Yikai Su

State Key Laboratory of Advanced Optical Communication Systems and Networks, Department of Electronic Engineering, Shanghai Jiao Tong University, Shanghai 200240, China

DOI:10.1109/JPHOT.2019.2920909

Manuscript received April 7, 2019; revised May 16, 2019; accepted May 31, 2019. Date of publication June 5, 2019; date of current version June 26, 2019. This work was supported in part by the National Key R&D Program of China under Grant 2016YFB0402501, in part by the National Natural Science Foundation of China (NFSC) under Grant 61875120, and in part by the Open Fund of IPOC (BUPT).
Corresponding author: Ciyuan Qiu (e-mail: qiuciyuan@sjtu.edu.cn).

Abstract: We propose and demonstrate a broadband silicon-based polarization beam splitter (PBS) by using cascaded tapered bent directional couplers (DCs). In our device, the TM-polarized light is efficiently cross coupled to the cross port due to the strong coupling in the DCs, while the TE-polarized light goes through the DC with weak coupling and outputs at the through port. This device can achieve a broad bandwidth performance and support *O*-, *S*-, *C*-, and *L*-band operations, with acceptable extinction ratios (ERs) and insertion losses (ILs). For both TE and TM polarizations, the simulation results show that ERs are $\geq$10.1 dB and ILs are $\leq$1.33 dB in 1280–1600 nm. In the measurement, for the TE polarization, an ER $\geq$10.94 dB and an IL $\leq$1.61 dB are obtained in 1280–1360 nm, while an ER $\geq$11.98 dB and an IL $\leq$1.39 dB are measured in 1510–1590 nm. For the TM polarization, an ER $\geq$12.25 dB and an IL $\leq$2.22 dB are obtained in 1280–1360 nm, while an ER $\geq$18.93 dB and an IL $\leq$1.22 dB are measured in 1510–1590 nm.

Index Terms: Polarization beam splitter, directional coupler, tapered waveguide.

1. Introduction

The polarization beam splitter (PBS) is a basic building block of silicon photonic circuits with polarization handling capability [1]. By using the compact PBS, one can utilize the polarization dimension of the transmitted light, and thus the data capacity for the on-chip optical system can be increased [2], [3]. Recently, various PBSs have been proposed and demonstrated based on photonic crystals [4], [5], multimode interference (MMI) structures [6], [7], directional couplers (DCs) [8], [9], Mach-Zehnder interferometer (MZI) structures [10] and grating-assisted contra-directional couplers (GACCs) [11].

In wide-band communication systems, it is highly desired to develop broadband PBSs with high extinction ratios (ERs) and low insertion losses (ILs). To satisfy the requirements, broadband PBSs have been demonstrated by using several structures, including bent DCs [8], [12]–[14] and tapered straight DCs [15]. Among the demonstrated broadband PBSs, bent DC-PBSs are regarded as attractive structures [8], due to their compact footprints, high stability and design simplicity. The ERs of the fabricated single bent DC-PBS are $>$10 dB for both TE-and TM- polarizations

in 1540 nm–1600 nm [12]. By cascading several bent DCs, the ER and IL performances of the PBS can be further improved, as well as the bandwidth performance [13], [14]. In [14], the ERs of such a PBS are 32.6 dB and 36.8 dB for the TE and TM polarizations, respectively, at the central wavelength of 1550 nm. Moreover, the bandwidths with ERs $>$10 dB for both two polarizations are measured to be $\sim$ 200 nm. To implement broadband PBSs, tapered straight DC is considered as another candidate structure since they can achieve broadband mode-coupling performance with high fabrication tolerance [16]. Recently, based on a straight tapered DC, a broadband PBS has been proposed and experimentally demonstrated [15]. For the fabricated tapered DC-PBS, an ER $>$16 dB and an IL $<$ 0.4 dB are obtained in a 100-nm wavelength range. These demonstrated DC-based PBSs have several advantages, including high ER, high fabrication tolerance and design simplicity. However, according to the measured results, their spectra are still not wide enough to support O-, S-, C- and L-band operations with high ERs, simultaneously.

By taking advantages of both bent DC-PBS and tapered DC-PBS, we have proposed a silicon-based PBS by a single tapered bent DC and presented preliminary simulation results, recently [17]. The DC consists of two tapered bent waveguides, whose widths are designed to satisfy the phase-matching condition for the TM polarization. Based on the simulation results, however, the operation band only covers the 1400 nm–1600 nm band which is still not wide enough.

To further increase the operation band, here we propose and experimentally demonstrate a silicon-based PBS by cascading two identical tapered bent DCs. Through a detailed study and a careful design for the parameters of the device, the PBS can work in a wide wavelength range and support O-, S-, C-, and L-band operations for optical communication. The simulation results show that ERs over 10.1 dB and ILs lower than 1.33 dB are obtained for both TE and TM light inputs in 1280 nm–1600 nm. In the measurements, limited by the laser sources, we evaluate the performance of the fabricated broadband PBS in 1280 nm–1360 nm and 1510 nm–1590 nm, respectively. For the TE polarization, an ER $\geq$10.94 dB and an IL $\leq$1.61 dB are obtained in 1280 nm–1360 nm, while an ER $\geq$11.98 dB and an IL $\leq$1.39 dB are measured in 1510 nm–1590 nm. For the TM polarization, an ER $\geq$12.25 dB and an IL $\leq$2.22 dB are obtained in 1280 nm–1360 nm while an ER $\geq$18.93 dB and an IL $\leq$1.22 dB are measured in 1510 nm–1590 nm. Our PBS achieves a good operation bandwidth with acceptable ER and IL performances on silicon platform.

2. Device Design and Principle

Fig. 1(a) illustrates the 3D schematic diagram for the ultra-broadband cascaded tapered bent DC-PBS. The device is built on a 220-nm-thick silicon-on-insulator (SOI) platform, covered with a SiO_2 upper cladding ($n_{Si} = 3.47$, $n_{SiO2} = 1.44$). It contains two identical tapered bent DCs with a total length of $\sim$32.74 μm. In each DC, the widths of the two waveguides are designed to be tapered as shown in Fig. 1(b), which stands in contrast to the traditional DC whose waveguides have fixed widths. In the coupling region of the DC, strong coupling for the TM-polarized light is designed. When the light signal with TM polarization is launched at the input port as shown in Fig. 1(a), it can be efficiently coupled to the bottom waveguide of the DC and then outputs at the cross port. Noted that, there is still residual TM-polarized light in the through port, which is then filtered out by a bent waveguide with a 3-μm radius (R_3). The ER for the TM polarization is then improved. Meanwhile, for the TE-polarized light input, the power coupling in the DC is weak. Thus, the light signal with TE polarization goes through the DC and outputs at the through port. However, partial power of the TE-polarization mode light will still be cross-coupled in the coupling region of DC #1. To improve the ER for the TE polarization, the second tapered bent DC-PBS (DC #2) is utilized to efficiently reduce the undesired cross-coupled TE-polarized power.

To obtain a strong coupling for the TM-polarized light in the DC and achieve a broadband performance, the phase-matching condition for the TM polarization should be satisfied in the coupling region of each DC [8]–[14]. Thus, for each DC, the parameters of the two waveguides and the gap between them are properly chosen. As shown in Fig. 1(b), the outer radius R_1 and the width of the initial part of the upper waveguide W_1 are set to 20 μm and 720 nm, respectively. And the gap is set to 100 nm. Then, the inner radius of the bottom waveguide R_2 can be determined by $R_2 = R_1 +$

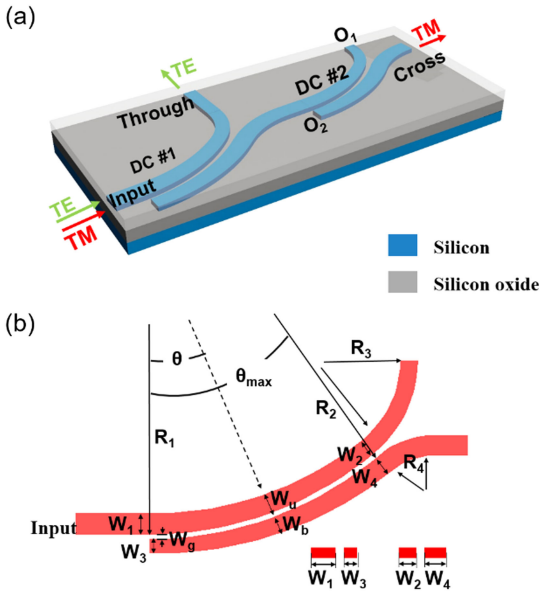

Fig. 1. Device configuration of the cascaded tapered bent DC-PBS (a) The 3D view; (b) The top view of a single DC. O_1 and O_2:Two unused output ports of DC #2.

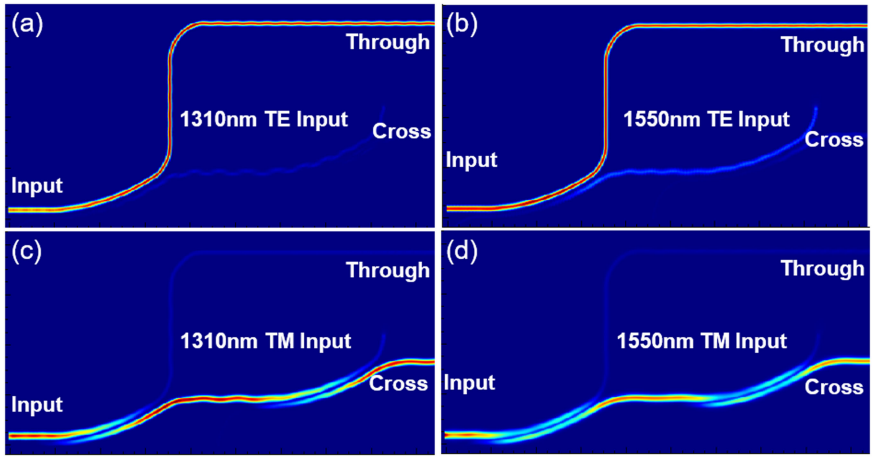

Fig. 2. Power distributions of the proposed DC-PBS (a) 1310 nm TE input; (b) 1550 nm TE input; (c) 1310 nm TM input; (d) 1550 nm TM input.

$W_g = 20.1\ \mu$m. The widths for both two waveguides are designed to tapered as shown in Fig. 1(b). For the upper waveguide, the waveguide width (W_u) gradually decreases from $W_1 = 720$ nm to $W_2 = 500$ nm, and W_u at a certain coupling angle θ can be expressed as $W_u = W_1 - (W_1 - W_2) \times \theta/\theta_{max}$. For the bottom waveguide, the waveguide width (W_b) gradually increases from $W_3 = 380$ nm to $W_4 = 620$ nm, and W_b at a coupling angle θ can be expressed as $W_b = W_3 + (W_4 - W_3) \times \theta/\theta_{max}$. Here the maximal angle (θ_{max}) is set to 30 degrees. Thus, the corresponding length of the coupling region, expressed as $R_1 \sin\theta_{max}$, is 13.22 μm. Moreover, the radius (R_4) for the bend of the bottom waveguide is set to 7 μm.

Figs. 2(a)–2(d) show the simulated power distributions of the device, by using the 3D finite-difference time-domain (FDTD) method. In the simulation, the mesh grid has a spatial resolution of

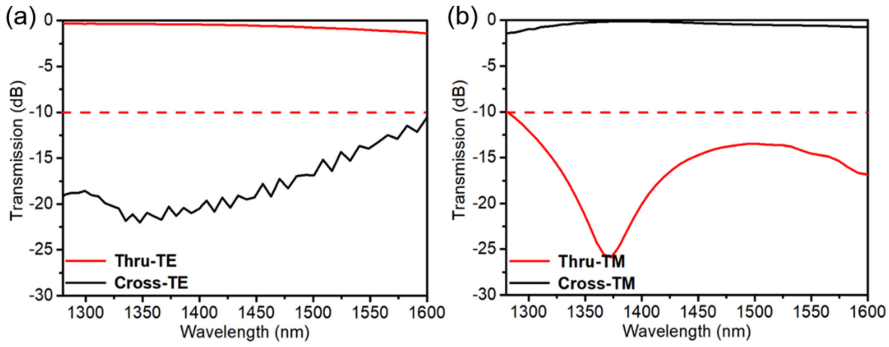

Fig. 3. Calculated transmission spectra at the cross- and through- ports of the PBS for the (a) TE-(b) TM-mode inputs.

$\sim$50 nm. From Figs. 2(a)–2(b), one can find that the TE_0 mode light at 1310 nm and 1550 nm goes straight in the upper waveguide and outputs at the through port. And the undesired cross-coupled power at the bottom waveguide is very weak. Meanwhile, when the light signal with TM polarization is launched, strong coupling is observed as shown in Figs. 2(c) and 2(d), for 1310 nm and 1550 nm, respectively. Most power of the TM_0 mode light is coupled to the bottom waveguide of the DC and outputs from the cross port. There is still some undesired TM-polarized light in the through port, which is then filtered out by the sharp waveguide bend. In addition, the TE-and TM-polarized lights at any wavelength of the whole operation bandwidth can be simulated and achieve similar results.

The calculated transmission spectra of the device for the TE-and TM-mode inputs are shown in Figs. 3(a) and 3(b), respectively. For TM polarization, one can find that a broad bandwidth performance with an ER $\geq$10.1 dB and an IL $\leq$1.37 dB is obtained in 1280 nm–1600 nm. Furthermore, for TE polarization, the ER is also $\geq$10.5 dB while the IL is $\leq$1.33 dB. For both polarizations, variations for the ER and IL can be found in the broad wavelength range, which can be attributed to the wavelength dependent property of the power coupling in the DC. Moreover, one can find oscillations of the TE-mode transmission at the cross port. This could be attributed to a weak Fabry-Perot (FP) interference from the reflections at the waveguide ends of two unused output ports O_1 and O_2, as shown in Fig. 1(a). The oscillations can be eliminated by integrating tapered waveguide structures at the waveguide ends of these two ports. Based on these calculated results, it can be noted that our proposed DC-PBS has a good bandwidth performance.

The fabrication tolerance of the designed PBS is also analyzed at the 1310 nm and 1550 nm, as shown in Figs. 4(a)–4(d). In the simulation, the two tapered waveguides of each DC are assumed to have the same width variation Δw due to fabrication errors and the center-to-center distance between the two tapered waveguides is fixed. From Figs. 4(a) and 4(b), optical transmissions at both through-and cross-ports do not experience significant degradations, when Δw changes from -10 nm to 20 nm. And ILs $\leq$1.5 dB and ERs $>$10 dB can be obtained for both two polarizations. However, when $\Delta w = -20$ nm, notable degradation is observed for the TM polarized light at 1310 nm. It can be attributed to the enlarged gap width W_g from the decreased waveguide widths, which significantly reduces the coupling efficiency for the TM polarized light at the shorter wavelength of 1310 nm.

Moreover, the device performance with respect to the outer radius (R_1) is also investigated. Broadband performance with low ILs and high ERs $\sim$ 10 dB for both two polarizations can still be obtained in 1280 nm–1600 nm if R_1 varies by $\pm$ 1 μm and W_g is set to 100 nm. However, if the variation of the radius is larger than 2 μm, the IL and ER would deteriorate since the radius variation changes the coupling length which has a strong influence on the light coupling efficiency.

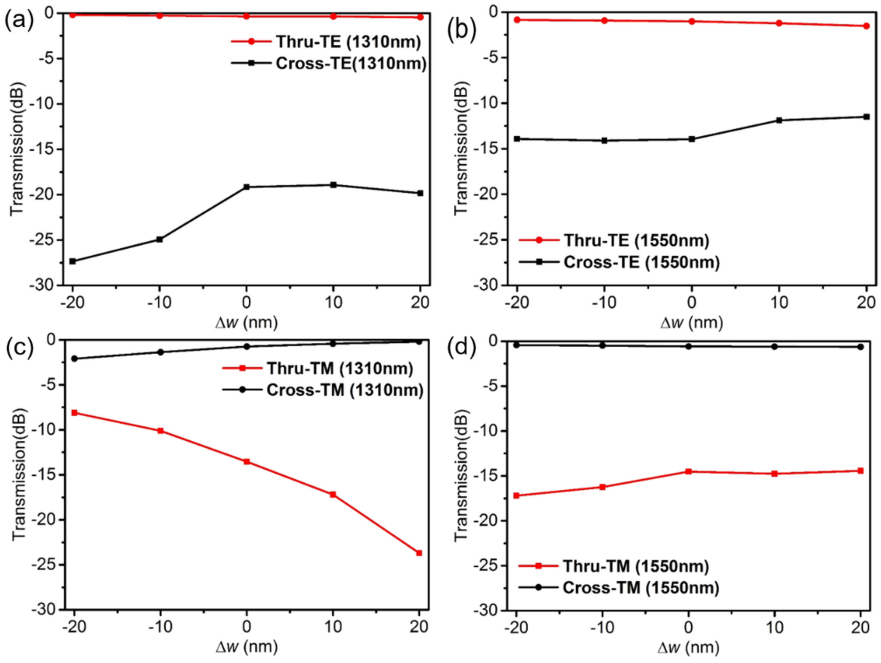

Fig. 4. Calculated optical transmissions at the cross- and through- ports of the PBS as a function of the waveguide width variation Δw (a) 1310 nm TE input; (b) 1550 nm TE input; (c) 1310 nm TM input; (d) 1550 nm TM input.

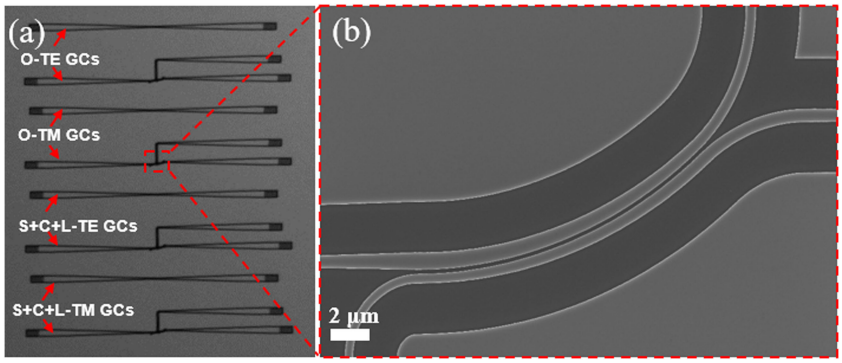

Fig. 5. (a) Microscope images of four identical PBSs with four kinds of grating couplers (GCs); (b) SEM image of a single DC of a PBS.

3. Fabrication, Experimental Setup and Results

The cascaded tapered bent DC-PBSs were fabricated on a SOI wafer with 220-nm-thick top silicon layer and 3-μm-thick buried SiO_2 layer. The device pattern was firstly defined on a positive electron-beam (E-beam) resist layer (ZEP-520) based on an E-beam lithography (EBL) process. Following the EBL process, an inductively coupled plasma (ICP) etching process was utilized to etch the top silicon and thus the pattern was transferred onto the silicon layer. Then, the E-beam resist layer was removed and then a 1-μm-thick SiO_2 layer was deposited as the cladding layer by plasma-enhanced chemical vapor deposition [11]. The microscope image of the devices with the different grating couplers (GCs) is shown in Fig. 5(a). And the zoom-in scanning electron microscope (SEM) image for the fabricated single DC of a PBS can be found in Fig. 5(b).

TABLE 1
Design Parameters and Measured Results of Grating Couples

Grating Couplers	Period(nm)	Filling factor	Coupling loss (dB)*	3-dB Bandwidth (nm)
O band TE	505	50.9%	6.5	37
O band TM	720	57.6%	6.9	32
C band TE	630	50%	5.6	45
C band TM	980	54.1%	5.9	43

*For each grating coupler, the measured coupling loss is obtained at its central wavelength.

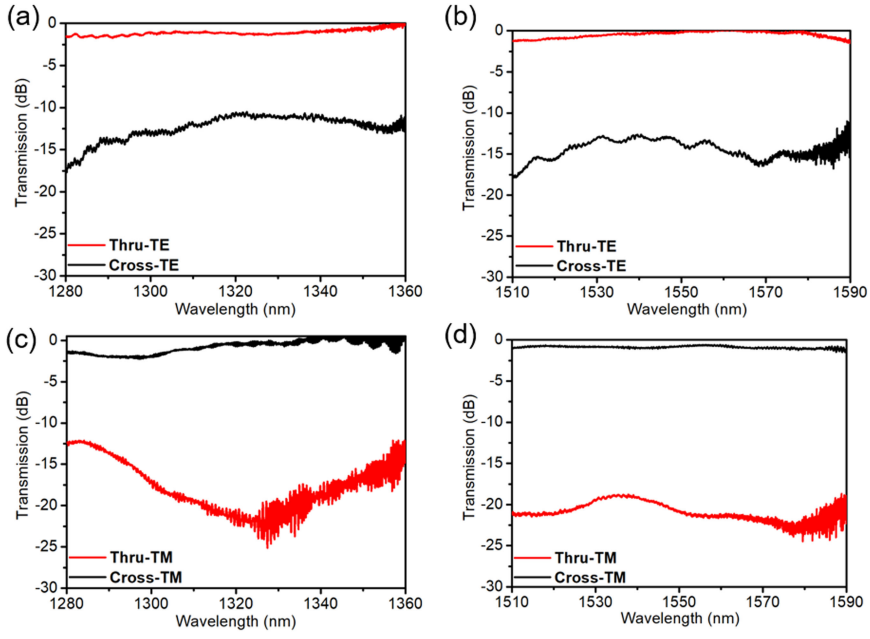

Fig. 6. Measured transmission responses of (a) O band TE input; (b) S+C+L band TE input; (c) O band TM input; (d) S+C+L band TM input.

In the measurement, O band (Santec TSL-550) and S+C+L band (Keysight 81960A) tunable continuous wave (CW) light sources were used to characterize the device performance in the wavelength ranges from 1280 nm–1360 nm and from 1510 nm–1590 nm, respectively. The polarization of light from the laser sources was adjusted to be TE-polarized or TM-polarized by a polarization controller (PC). Then the light was injected into the chip through grating couplers (GCs). After passing through the devices, the output light power at through- and cross- ports was recorded by an optical power meter. Since grating couplers have a passband and polarization dependent performance, four identical PBSs were fabricated with four kinds of grating couplers to evaluate the device performance in two wavelength bands (O band and S+C+L band) and at two different polarizations (TE and TM), respectively, as shown in Fig. 5(a). Design parameters as well as measured coupling losses and 3-dB bandwidths for the four kinds of grating couplers are provided in the Table 1. The etching depth for all grating couplers is 70 nm.

TABLE 2
Comparisons of Various Reported DC-PBSs

Structure	Bandwidth （nm）	ER(dB)	IL(dB)	Supporting band
Bent waveguide [8] (simulated)	~200	> 10	N/A	S+C+L
Slot waveguide [9] (simulated)	160	> 10	N/A	S+C+L
Cascaded Bent DCs [14] (experimental)	~135	> 20	< 1	S+C+L
Tapered straight DC-PBS[15] (experimental)	100	> 16	< 0.4	S+C+L
Triple bent DC-PBS [19] (experimental)	90	> 20	< 2	S+C+L
Bridged structure [20] (experimental)	100	> 20	< 2.1 (@1550 nm)	S+C+L
Our work (simulated)	320	≥ 10.1	≤1.33	O+S+C+L
Our work (experimental)	160	> 10	≤ 2.22(O) ≤ 1.39 (S+C+L)	O+S+C+L

Figs. 6(a)–6(d) show the measured transmission spectra of the bent tapered DC-PBSs. For the TE polarization over 1280 nm–1360 nm, light goes through at the through port with an ER ≥10.94 dB and an IL ≤1.61 dB, as shown in Fig. 6(a). And an ER ≥11.98 dB and an IL ≤1.39 dB are obtained in the 1510 nm–1590 nm band as show in Fig. 6(b). For the TM polarization over 1280 nm–1360 nm, light is efficiently coupled to the cross port with an ER ≥12.25 dB and an IL ≤2.22 dB, as shown in Fig. 6(c). And an ER ≥18.93 dB and an IL ≤1.22 dB are obtained in the 1510 nm–1590 nm band as shown in Fig. 6(d). One can find that the measured spectra almost agree with those in simulations while the measured IL in the O band for the TE polarization is a little larger than that in simulation, which may be due to the fabrication issues. Furthermore, thanks to the structure of tapered bend waveguide, the measured spectra are almost flat in the two wavelength bands. This is different from the measured spectra of the previous demonstrated PBSs, which have a maximal ER and a minimal IL at the central wavelength. Meanwhile, it can be observed that there are power variations when the wavelength λ>1330 nm and λ>1580 nm, due to the detection sensitivity and the operation bandwidths of grating couplers. Based on these above experimental results, our PBS shows a broadband performance of ~80 nm and ~80 nm at the O- and S+C+L-bands, respectively.

Table 2 compares our device with various silicon-based DC-PBSs. It indicates that, our cascaded tapered bent DC-PBS has a wide bandwidth in simulation and the ability to support O-, S-, C- and L-band operations in experiment, which can have potential applications in coarse wavelength division multiplexer (CWDM) systems [18].

4. Conclusion

In summary, we propose and successfully demonstrate a broadband silicon-based PBS by using cascaded tapered bent directional couplers, which supports O-, S-, C-, and L- band operations, simultaneously. According to the simulated results, ERs ≥10.1 dB and ILs ≤1.33 dB are obtained for both the TE and TM inputs over a broad wavelength range of 320 nm (1280 nm–1600 nm). In the experiment, we characterized the device performances in the wavelength ranges from 1280 nm

to 1360 nm and from 1510 nm to 1590 nm, limited by the laser sources. Based on the measured data, the device has relative high ERs ($>$10 dB) and low ILs in the whole tested wavelength range for both two polarizations. To further improve the ER, one can cascade a TE-pass polarizer [21] at the through port and a TM-pass polarizer [22] at the cross port to effectively reduce unwanted polarized light powers at the two ports, respectively. Moreover, from the flat measured transmission spectra in the two wavelength bands, low ILs and high ERs are expected for both two polarizations in the unmeasured wavelength range from 1360 nm to 1510 nm, due to optical characteristics of DC-based devices. Thus, our device could support O-, E-, S-, C- and L- band operations, according to the simulation and experimental results.

References

[1] B. Shen, P. Wang, R. Polson, and R. Menon, "An integrated-nanophotonics polarization beamsplitter with 2.4 $\times$ 2.4 μm^2 footprint," *Nature Photon.*, vol. 9, no. 6, pp. 378–382, Jun. 2015.

[2] P. Dong, X. Liu, S. Chandrasekhar, L. L. Buhl, R. Aroca, and Y. K. Chen, "Monolithic silicon photonic integrated circuits for compact 100(+)Gb/s coherent optical receivers and transmitters," *IEEE J. Sel. Topics Quantum Electron.*, vol. 20, no. 4, Jul./Aug. 2014, Art. no. 6100108.

[3] P. Dong, X. Chen, K. Kim, S. Chandrasekhar, Y. K. Chen, and J. H. Sinsky, "128-Gb/s 100-km transmission with direct detection using silicon photonic Stokes vector receiver and I/Q modulator," *Opt. Exp.*, vol. 24, no. 13, pp. 14208–14214, Jun. 2016.

[4] T. Liu, A. R. Zakharian, M. Fallahi, J. V. Moloney, and M. Mansuripur, "Design of a compact photonic-crystal-based polarizing beam splitter," *IEEE Photon. Technol. Lett.*, vol. 17, no. 7, pp. 1435–1437, Jul. 2005.

[5] X. Y. Ao, L. Liu, L. Wosinski, and S. L. He, "Polarization beam splitter based on a two-dimensional photonic crystal of pillar type," *Appl. Phys. Lett.*, vol. 89, Oct. 2006, Art. no. 171115.

[6] B. M. A. Rahman, N. Somasiri, C. Theimistos, and K. T. V. Grattan, "Design of optical polarization splitters in a single-section deeply etched MMI waveguide," *Appl. Phys. B, Lasers Opt.*, vol. 73, no. 5/6, pp. 613–618, Oct. 2001.

[7] Y. H. Ding, H. Y. Ou, and C. Peucheret, "Wideband polarization splitter and rotator with large fabrication tolerance and simple fabrication process," *Opt. Lett.*, vol. 38, no. 8, pp. 1227–1229, Apr. 2013.

[8] D. X. Dai and J. E. Bowers, "Novel ultra-short and ultra-broadband polarization beam splitter based on a bent directional coupler," *Opt. Exp.*, vol. 19, no. 19, pp. 18614–18620, Sep. 2011.

[9] D. X. Dai, Z. Wang, and J. E. Bowers, "Ultrashort broadband polarization beam splitter based on an asymmetrical directional coupler," *Opt. Lett.*, vol. 36, no. 13, pp. 2590–2592, Jul. 2011.

[10] T. K. Liang and H. K. Tsang, "Integrated polarization beam splitter in high index contrast silicon-on-insulator waveguides," *IEEE Photon. Technol. Lett.*, vol. 17, no. 2, pp. 393–395, Feb. 2005.

[11] Y. Zhang *et al.*, "High-extinction-ratio silicon polarization beam splitter with tolerance to waveguide width and coupling length variations," *Opt. Exp.*, vol. 24, no. 6, pp. 6586–6593, Mar. 2016.

[12] J. Wang, D. Liang, Y. B. Tang, D. X. Dai, and J. E. Bowers, "Realization of an ultra-short silicon polarization beam splitter with an asymmetrical bent directional coupler," *Opt. Lett.*, vol. 38, no. 1, pp. 4–6, Jan. 2013.

[13] H. Wu and D. X. Dai, "High-performance polarizing beam splitters based on cascaded bent directional couplers," *IEEE Photon. Technol. Lett.*, vol. 29, no. 5, pp. 474–477, Mar. 2017.

[14] H. Wu, Y. Tan, and D. X. Dai, "Ultra-broadband high-performance polarizing beam splitter on silicon," *Opt. Exp.*, vol. 25, no. 6, pp. 6069–6075, Mar. 2017.

[15] D. G. Chen, X. Xiao, L. Wang, G. Gao, W. Liu, and Q. Yang, "Broadband, fabrication-tolerant polarization beam splitters based on a tapered directional coupler," *IEEE Photon. Technol. Lett.*, vol. 28, no. 19, pp. 2074–2077, Oct. 2016.

[16] M. G. F. Wilson and G. A. Teh, "Tapered optical directional coupler," *IEEE Trans. Microw. Theory Techn.*, vol. 23, no. 1, pp. 85–92, Jan. 1975.

[17] N. Zhao, Y. He, C. Y. Qiu, Y. Zhang, and Y. K. Su, "Ultra-broadband polarization beam splitter based on a tapered bent directional coupler," in *Proc. Asia Commun. Photon. Conf.*, 2018, pp. 1–3, doi: 10.1109/ACP.2018.8596254.

[18] I. H. White *et al.*, "Optical local area networking using CWDM," *Semicond. Optoelectron. Devices Lightw. Commun.*, vol. 5248, pp. 284–293, 2003.

[19] J. R. Ong *et al.*, "Broadband silicon polarization beam splitter with a high extinction ratio using a triple-bent-waveguide directional coupler," *Opt. Lett.*, vol. 42, no. 21, pp. 4450–4453, Nov. 2017.

[20] D. W. Kim, M. H. Lee, Y. Kim, and K. H. Kim, "Planar-type polarization beam splitter based on a bridged silicon waveguide coupler," *Opt. Exp.*, vol. 23, no. 2, pp. 998–1004, Jan. 2015.

[21] Y. L. Xiong, D. X. Xu, J. H. Schmid, P. Cheben, and W. N. N. Ye, "High extinction ratio and broadband silicon TE-pass polarizer using subwavelength grating index engineering," *IEEE Photon. J.*, vol. 7, no. 5, Oct. 2015, Art. no. 7802107.

[22] X. W. Guan, P. X. Chen, S. T. Chen, P. P. Xu, Y. C. Shi, and D. X. Dai, "Low-loss ultracompact transverse-magnetic-pass polarizer with a silicon subwavelength grating waveguide," *Opt. Lett.*, vol. 39, no. 15, pp. 4514–4517, Aug. 2014.